Luca D'Andrea
Department of Chemistry, Materials and Chemical Engineering Giulio Natta, Politecnico di Milano, Milano 20133, Italy
e-mail: luca.dandrea@polimi.it

Maddalena Cardamone
Department of Chemistry, Materials and Chemical Engineering Giulio Natta, Politecnico di Milano, Milano 20133, Italy
e-mail: maddalena.cardamone@mail.polimi.it

Francesca Bogoni
Department of Chemistry, Materials and Chemical Engineering Giulio Natta, Politecnico di Milano, Milano 20133, Italy
e-mail: francesca.bogoni@mail.polimi.it

Elisa Forzinetti
Department of Chemistry, Materials and Chemical Engineering Giulio Natta, Politecnico di Milano, Milano 20133, Italy
e-mail: elisa.forzinetti@mail.polimi.it

Viviana Enei
Department of Chemistry, Materials and Chemical Engineering Giulio Natta, Politecnico di Milano, Milano 20133, Italy
e-mail: viviana.enei@mail.polimi.it

Francesco Valle
CORCYM, Saluggia 13040, Italy
e-mail: Francesco.Valle@corcym.com

Giovanni Giordano
CORCYM, Saluggia 13040, Italy
e-mail: Giovanni.Giordano@corcym.com

Dario Gastaldi
Department of Chemistry, Materials and Chemical Engineering Giulio Natta, Politecnico di Milano, Milano 20133, Italy
e-mail: dario.gastaldi@polimi.it

Pasquale Vena
Department of Chemistry, Materials and Chemical Engineering Giulio Natta, Politecnico di Milano, Milano 20133, Italy
e-mail: pasquale.vena@polimi.it

Anisotropic Mechanical Response of Bovine Pericardium Membrane Through Bulge Test and In-Situ Confocal-Laser Scanning

In this work, we present a new experimental setup for the assessment of the anisotropic properties of Bovine Pericardium (BP) membranes. The chemically fixed BP samples have been subjected to a bulge test with in situ confocal laser scanning at increasing applied pressure. The high resolution topography provided by the confocal laser scanning has allowed to obtain a quantitative measure of the bulge displacement; after polynomial fitting, principal curvatures have been obtained and a degree of anisotropy (DA) has been defined as the normalized difference between the maximum and minimum principal curvatures. The experiments performed on the BP membranes have allowed us to obtain pressure-displacement data which clearly exhibit distinct principal curvatures indicating an anisotropic response. A comparison with curvatures data obtained on isotropic Nitrile Buthadiene Rubber (NBR) samples has confirmed the effectiveness of the experimental setup for this specific purpose. Numerical simulations of the bulge tests have been performed with the purpose of identifying a range of constitutive parameters which well describes the obtained range of DA on the BP membranes. The DA values have been partially validated with biaxial tests available in literature and with suitably performed uni-axial tensile tests. [DOI: 10.1115/1.4056398]

1 Introduction

Bovine pericardium (BP) is a collagenous tissue which is largely adopted for the manufacturing of bioprosthetic heart valves (BHVs) [1]. This material shows a time dependent and a nonlinear stress/strain response [2,3]. Prior to be used for medical purposes, the tissue is sterilized and it is rendered inert by chemical fixation with glutaraldehyde. Indeed, glutaraldehyde-fixed bovine pericardium (GLBP) is employed in six of nine CE-marked BHV devices [4].

Bovine pericardium membranes contain a small amount of elastin and multidirectional bundles of collagen embedded in an amorphous matrix which induce mechanical anisotropy. The

Manuscript received June 8, 2022; final manuscript received November 28, 2022; published online January 11, 2023. Assoc. Editor: Kyle Quinn.

collagen fibers, primarily of type I, have a preferential directionality and constitute the main component of the tissue [3,5,6]. As the collagen fibers are the major load bearing components, their arrangement determines the mechanical response of the tissue upon loading [1,4,5].

Despite the relevance of the collagen network on the mechanical anisotropy of BP membranes, the standard ISO 5840 for the design and manufacture of prosthetic heart valves does not require to characterize the collagen fiber architecture and to identify their preferential direction [4]. Therefore, BHVs are generally not designed to exploit the tissue anisotropy in a systematic way [6]. This has important implications in the performance of BHV leaflets, whose fatigue life can be significantly reduced if design of the device does not account for principal material directions. Moreover, the orientation and the alignment of the fibers with respect to the in vivo loading directions are two critical factors to prevent the onset of mechanical damage and to delay and minimize the calcification [7].

In previous studies, BP has been characterized mainly through in plane and out of plane mechanical tests [8]. As for the in-plane tests, the BP has been investigated by means of uni-axial mechanical tests, both static [1,4,9,10] and cyclic [1,4], and through biaxial stretching [9–13]. For what concerns the out of plane mechanical tests, bulge test can be used. In this case, the membrane is subjected to a pressure on its surface representing a more realistic mimicking of the in vivo loading conditions [14,15]. Nevertheless, this test has been used to investigate the properties of BP only in a few studies: Zioupos et al. [2] have studied the anisotropy of the tissue while Whelan et al. [16] have investigated the correlation between the collagen fibers dispersion and the fatigue life.

The identification of the preferential directions of the collagen fibers and of the degree of anisotropy can be performed through direct and indirect experimental methods. Examples of direct methods are multiphoton microscopy [14,15], small angle light scattering [1,4,12,16] or polarimetric fiber alignment imaging [17]. While, indirect methods are typically based on digital image correlation (DIC) [16,18] or Moirè fringes production [2].

The aim of this study is to evaluate the degree of anisotropy of GLBP membranes through a mechanical bulge test and simultaneous confocal laser microscopy.

Furthermore, the experimental scenario has been also represented through a finite element model with the purpose to determine ranges for constitutive parameters with particular reference to the anisotropic properties of the tissue. The degree of anisotropy found through bulge experiments has been partially validated by means of suitably developed uni-axial tensile tests.

2 Materials and Methods

2.1 Material Samples. The samples of BP have been fixed in a 0.5% glutaraldehyde solution for 72 h; subsequently patches with size 50 × 50 mm have been cut and stored in a bacteriostatic solution (Steridet®). The thickness of each patch has been measured in three points picked in the central region by means of a caliper and the average thickness has been determined; the patches have been then grouped in thickness classes as follows:

(1) 0.4 – 0.5 mm: 10 samples characterized by an average thickness of 0.44 ± 0.03 mm
(2) 0.5 – 0.6 mm: 18 samples characterized by an average thickness of 0.55 ± 0.03 mm
(3) 0.6 – 0.7 mm: 9 samples characterized by an average thickness of 0.65 ± 0.02 mm

2.2 Experimental Setup: The Bulge Test. The bulge test setup is composed by: a bulge test device and a pressure delivery system. The bulge device is composed by an upper and a lower die; these are aluminum parallelepipeds with a cross-sectional area of 90 × 90 mm and a thickness of 5 mm. A circular bulge window (ø = 30 mm) is located in the center of each die. The two dies are tightened by means of eight bolts. O-rings ($ø_i$ = 40 mm, $ø_e$ = 44 mm) are used to guarantee a water-proof system. The first o-ring is positioned at the interface between the BP and the lower die, while the second one is placed between the cylindrical connector and the water chamber (Fig. 1).

The pressure on the lower surface of the BP is provided by means of a water column; the pressure is controlled by changing the height of the water in the column. The lower die has a cylindrical connector to host a PVC chamber in which the water is collected. This component has an external diameter of 40 mm, an height of 40 mm and a thickness of 5 mm. In the lower part of the chamber there is a circular hole (ø = 6 mm) in which a tube, used to connect the device to the water column, is inserted. Once the water column is connected to the bulge test device, the water fills the circuit, according to the communicating vases system. The system is filled with water before the BP membrane is put in place in order to eliminate air in the circuit. The BP is positioned on the lower die, covering the first o-ring and the upper die is placed upon it. As soon as the bolts are sufficiently tightened, the device is positioned on the confocal microscope tray. After bolts tightening, the membrane gets compressed and, owing to its nearly incompressible response, a nonplanar configuration is observed within the circular window. A tiny initial water pressure of 0.1 kPa is delivered to the sample in order to obtain a configuration characterized by a uniform curvature. This configuration is considered as a reference shape for subsequent displacement measurements.

The bulge test is performed by a progressive stepwise increase of the water pressure, with increments of 0.1 kPa until water leakage through the BP membrane, owed to the intrinsic tissue permeability, is observed.

Two isotropic membranes of Nitrile Buthadiene Rubber (NBR) material have been tested following the same procedure, with the purpose to test the efficacy of the anisotropy assessment.

2.3 Experimental Setup: The Confocal Laser Scanning Microscopy. High resolution three-dimensional topography of the top BP surface within the circular hole has been obtained using a confocal laser scanning microscope (LEXT OLS4100, Olympus, Tokyo, Japan) with a laser wavelength of 406 nm. The laser scans have been performed at the initial pressure 0.1 kPa and at each pressure level in the stepwise load program.

The acquisitions have been performed with a 5× lens, a long-distance objective (20 mm) with a field of view (FOV) of 2560 μm. As a creep behavior is expected for biological membranes, a steady-state condition has been first attained by setting a 3 min holding time before acquisition. A three dimensional high resolution topography has been obtained by imaging and setting the objective lenses at multiple z-positions with a separation of acquisition planes along the z-direction of 20 μm; this separation is a compromise between resolution and timing; the resolution in the vertical direction is equal to 10 μm, while the one in the plane is equal to 2.5 μm.

Since the FOV of the selected objective is insufficient to capture the behavior of a significant portion of the tissue, a stitching procedure has been performed by acquiring subregions (2560 × 2560 μm) and subsequently merging different images with the aim of having one larger single image (12 × 12 mm) with the same resolution as that obtained on the single subregion. The matrix (5 × 5) of subregions on which the stitching is performed has been placed in the center of the circular window, prior to the first acquisition, and it has been kept constant for all pressure levels.

2.4 Experimental Data Analysis. The confocal laser microscope provides a high resolution topography as a cloud of points for each pressure level of the test. The cloud of points is in the

form $z(x, y)$ in which z is the vertical position of a point of the surface with respect to a reference plane, this latter being the same for all pressure levels; while x and y are the surface point positions on the horizontal plane. At the start of each test, a high resolution map of a portion of the top die has been also performed with the aim to determine and correct potential tilting of the images.

Subsequent experimental data analyses have been performed by means of suitably developed MATLAB code (MATLAB 2021). The cloud of points in the form $z(x, y)$ has been interpolated by using fourth order polynomial functions $f^i(x, y, p^i)$, in which p^i is the i-th pressure level. Cartesian curvatures have been obtained through second order numerical derivative:

$$\chi^i_{xx} = \frac{\partial^2 f^i(x,y,p^i)}{\partial x^2}; \quad \chi^i_{yy} = \frac{\partial^2 f^i(x,y,p^i)}{\partial y^2}; \quad \chi^i_{xy} = \frac{\partial^2 f^i(x,y,p^i)}{\partial x \partial y} \tag{1}$$

Principal curvatures $\chi^i_{\max}$ and $\chi^i_{\min}$ have been obtained by finding eigenvalues of Eq. (1). The degree of anisotropy (DA) has been defined as:

$$\mathrm{DA}^i = \frac{(\chi_{\max} - \chi_{\min})}{\chi_{\min}}\bigg|_i \tag{2}$$

in which $\chi_{\max}$ and $\chi_{\min}$ are the principal curvatures calculated at the point where the maximum displacement is found. Isotropic membranes are expected to have $\mathrm{DA} = 0$; while anisotropic response is characterized by $\mathrm{DA} > 0$.

The maximum vertical displacement has also been determined at each pressure level ($z^i_{\max}$). As the configuration at pressure 0.1 kPa is considered as a reference, for each pressure level, the relative vertical displacement Δz^i has been computed as follows:

$$\Delta z^i = z^i_{\max} - z^0_{\max} \tag{3}$$

in which $z^0_{\max}$ is the maximum displacement found at $p = 0.1$ kPa.

2.5 Statistical Analysis. A normality test (Kolmogorov–Smirnov) has been run for each experimental dataset (pressure level and thickness group); displacement data and DA data have been analyzed.

Significant statistical differences have been tested by means of the Mann–Whitney test for the three classes of thickness, compared at groups of two.

2.6 Uni-axial Tensile Tests for the Validation of the Degree of Anisotropy. In order to have a partial independent validation of the DA assessed through the bulge test and confocal laser scanning, uni-axial tensile tests have been performed on rectangular samples of a pericardium membrane, and a DA has been determined.

Rectangular samples (25 mm × 5 mm) have been cut using a blade from square patches 50 mm × 50 mm. Thickness of the samples has been measured following the same procedure as the one described above.

In order to determine the principal material directions, preliminary tests have been made on samples oriented along four different orientations. The principal material directions have been identified by selecting the orientation for the stiffest response and the perpendicular one. Uni-axial tensile tests have been performed using two 15 mm translational stages, with DC gear motor and a high resolution encoder (M-111-1DG1, 200 nm motion resolution, Physik Instrumente, Karlsruhe, Germany); a load cell of 50 N maximum load and 0.1% of nominal sensitivity (model 8417-5050, Burster) has been used to measure the force. The samples have been subjected to two opposite longitudinal displacement so to have the central part of the sample in a steady position during the test below the objective of a microscope. All tests have been run keeping the sample in wet conditions.

The strain in the central part of sample has been estimated by means of the DIC. To this purpose, a pattern is realized by means of an airbrush using a water-based black tint, specific for the airbrush usage (procolor #61024 HANSA®). The pattern has been observed throughout the test by means of the stereomicroscope SZ61TR, by Olympus. A region of interest has been selected on the pattern and an average strain along the loading direction has been assessed through the open source two-dimensional package Ncorr. An average value on the 5 mm × 2.5 mm region of interest has been obtained using the large strain formulation.

The DA in uni-axial tensile data has been determined similarly to Eq. (2) as:

$$\mathrm{DA} = \frac{|\sigma_{\max} - \sigma_{\min}|}{\sigma_{\min}} \tag{4}$$

at different strain levels.

2.7 Finite Element Modeling of the Bulge Test. A finite element model of the experiments has been developed by using the commercial code ABAQUS.

The model is composed of three parts: the upper die, the BP membrane and the lower die. The two dies are modeled as parallelepipeds with a square section (90 × 90 × 5 mm) having a central circular hole (ø= 30 mm). The two parts are defined as rigid bodies, meshed with 10185 shell elements of types R3D3 and R3D4. The patch of BP is represented as a parallelepiped with a square shape (50 × 50 × 0.5 mm), defined as a deformable three dimensional solid, meshed with 53280 elements of type C3D8H. Six elements through the thickness direction have been used.

The stress–strain relationship for the BP elements has been described through the constitutive model of Holzapfel-Gasser-Ogden (HGO) [19]. One single family of fibers and an orientation dispersion parameter κ have been used.

The HGO model [19] is defined through the strain energy function of a fiber reinforced composite which depends on 4 constitutive parameters: C_{10} accounting for energy stored in the isotropic matrix; k_1 and k_2 accounting for the energy stored in the fibers and κ accounting for a statistical dispersion of fibers orientation in space. This latter parameter ranges in the domain $0 < \kappa < 1/3$, where $\kappa = 0$ corresponds to the deterministic orientation of the family of fibers (no dispersion) and $\kappa = 1/3$ represents a random fiber orientation thus resulting in an isotropic material response.

A surface-to-surface contact has been applied between each die and the patch of BP. This contact is characterized by a tangential behavior with penalty ($\mu_s = 0.2$) and a hard contact normal behavior.

Since the dies are defined as rigid bodies, their motion is driven through reference points. The lower die has been fully constrained to the reference system. Three steps are defined in this simulation:

(1) *Tightening*: a displacement of 0.1 mm (20% of the thickness of the sample) is applied to the reference point of the upper die to reproduce the tightening of the bolts;
(2) *Minimum pressure*: a uniform minimum pressure of 0.1 kPa is applied to the bottom surface of the BP. This is the initial reference pressure;
(3) *Maximum pressure*: to simulate the inflation of the specimen, a uniform maximum pressure of 2 kPa is applied on bottom surface of the BP.

For each simulation, the two coordinates in the plane of BP and the vertical displacement in a square region defined at the center

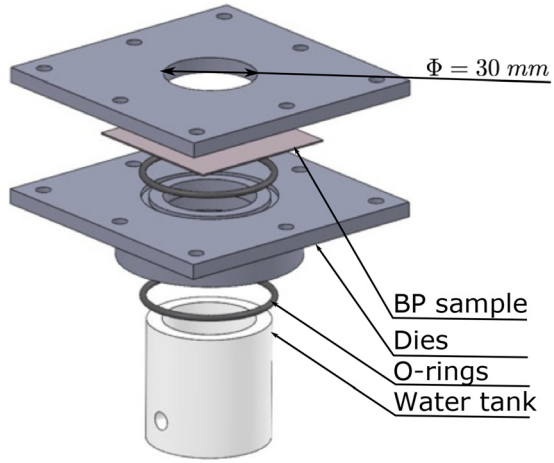

Fig. 1 Bulge test device

of the circular window (14 × 14 mm) have been obtained. These data have then been treated as pseudo-experimental data and have been analyzed using the same methods described in Sec. 2.4.

3 Results

3.1 Experimental Results. Figure 2 (top) shows the relative displacement as a function of the incremental pressure (reference value for pressure is $p^0 = 0.1$ kPa); the average values for each thickness class have been reported along with an error bar at each pressure level. As expected a nonlinear pressure-displacement response has been found with increasing slope at increasing displacement. Thicker BP samples have exhibited lower displacement at a given pressure level. The maximum Δz has been found to be approx. 1.1 mm at $\Delta p = 0.5$ kPa for the thinnest class of BP; while the thickest membranes have achieved a maximum $\Delta z = 1$ mm at $\Delta p = 0.9$ kPa.

The Kolmogorov–Smirnov test has shown that all dataset cannot be represented with a normal statistical distribution.

The Mann–Whitney test has shown that statistical differences (p-value < 0.05) for the maximum displacement have been found among the different thickness classes; in particular, p-values are reported in Table 1.

Figure 2 (bottom) shows the DA parameter as a function of the pressure increment, for all classes of thickness. The statistical tests have shown that no statistical difference among different thickness class is found.

3.2 Uni-Axial Tensile Tests and Validation of Degree of Anisotrophy Results. A comparison of the DA found on bulge tests with that found on: (i) uni-axial test data obtained in this study and (ii) biaxial test data reported in Ref. [12] is here presented. In both uni-axial and biaxial test data, the DA parameter has been assessed through Eq. (4).

Figure 3 shows the stress–strain average data and standard deviation of uni-axial tensile tests along the two principal material directions. At 25%, strain standard deviation is approximately 47% for the stiffest curve and 16% for the softest curve.

Figure 4 shows the value of DA as a function of strain. DA found in uni-axial and biaxial tests have been reported with blue crosses and red circles, respectively. The DA obtained from bulge test has been reported at the representative strain of 2.6% approximately achieved at the maximum applied pressure before water leaks through the membrane. Both the DA from biaxial tests [12] and from uni-axial tests show a decreasing trend up to a strain of 5% followed by an increasing DA. The DA from uni-axial tests is slightly lower than that found in biaxial testing. The DA obtained through the bulge tests is consistent with that found in biaxial tests and higher than that found in unixial tests. The average DA in uni-axial testing falls within the error bar of the DA obtained through bulge.

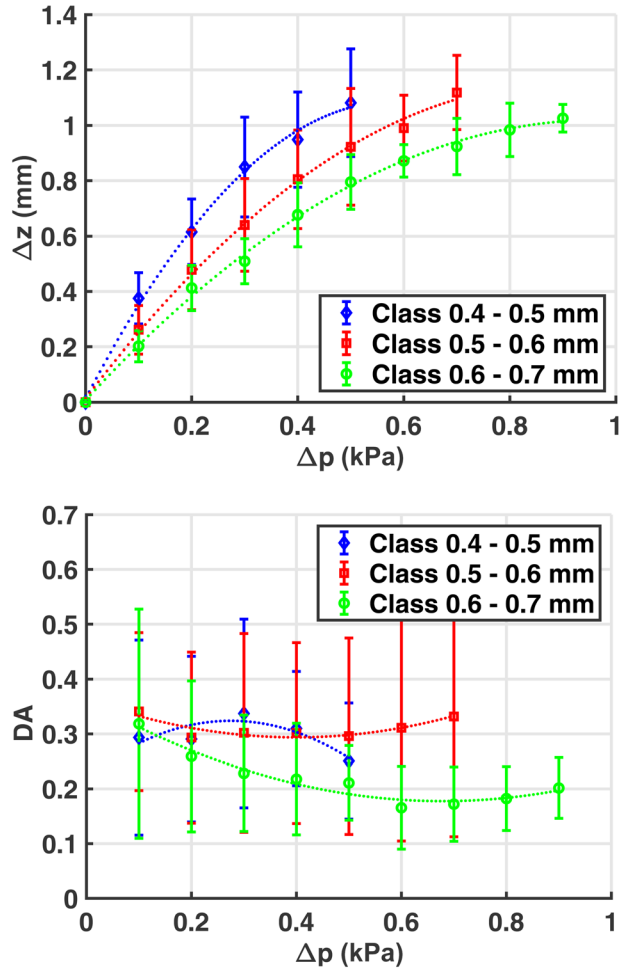

Fig. 2 Top panel: maximum relative displacement versus pressure increment; bottom panel: Degree of Anisoptropy versus pressure increment. Different colors refer to different thickness classes.

3.3 Numerical Simulation of the Bulge Experiments. A trial and error procedure has been used to fit finite element results with the experimental data in terms of relative displacement versus incremental pressure and DA. For each class of BP thickness, the displacement results exhibit a substantially lower scatter of data with respect to that exhibited by the DA data (see Fig. 2). Therefore, for each class of thickness, the sets of constitutive

Table 1 *p*-values for maximum relative displacement comparison between thickness groups (thickness in [mm]); *p*-values for significant difference are reported in boldface

Δp (kPa)	0.4–0.5 versus 0.5–0.6	0.4–0.5 versus 0.6–0.7	0.5–0.6 versus 0.6–0.7
0.1	**0.0156**	**0.0024**	0.0948
0.2	**0.0445**	**0.0045**	0.2357
0.3	**0.0156**	**0.0011**	**0.0289**
0.4	0.1092	**0.0045**	**0.0356**
0.5	0.11512	**0.0028**	0.1092
0.6	—	—	**0.01**
0.7	—	—	**0.0049**

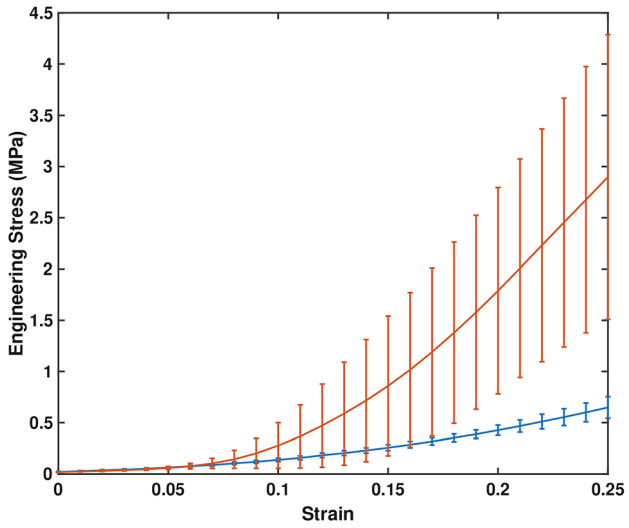

Fig. 3 Stress-strain response in uni-axial tests along the two principal direction of the material; error bars indicate standard deviation

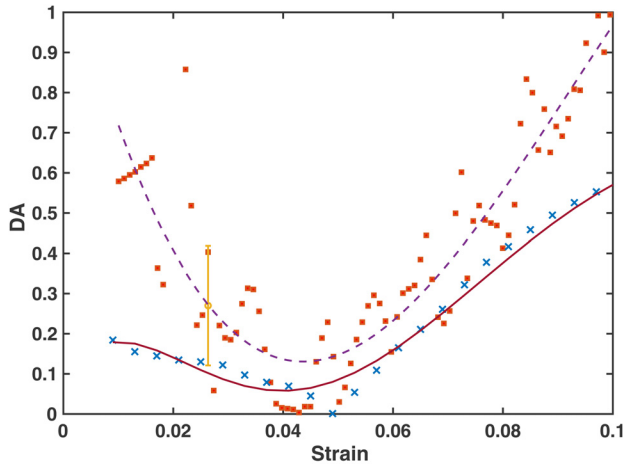

Fig. 4 Degree of anisotropy versus strain: Uni-axial tensile tests (blue circles); Biaxial stretching from Sacks et al. [12] (red circles), a polynomial fitting is also reported; Bulge tests: orange symbol with error bar

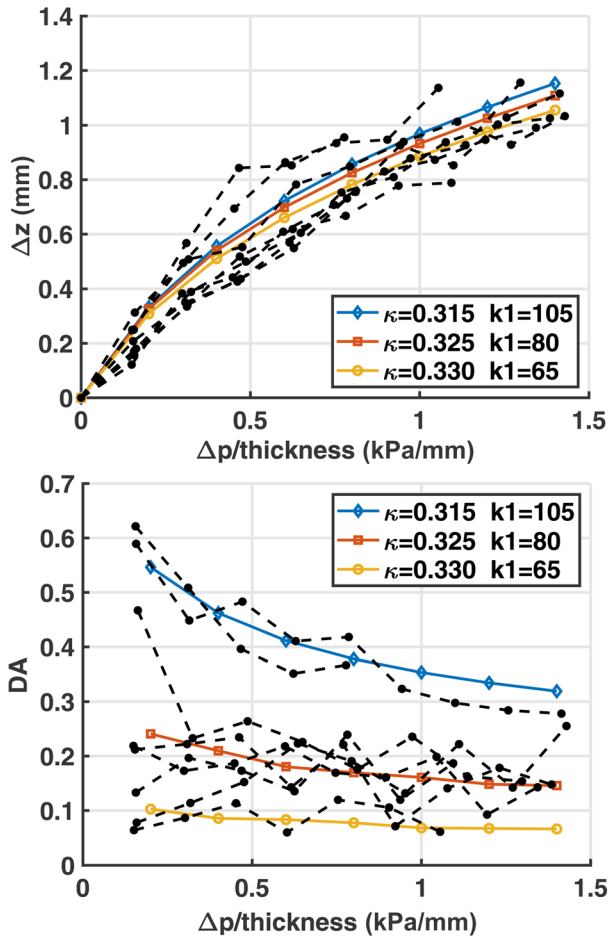

Fig. 5 Experimental results (0.6−0.7 mm) compared with finite element results covering the whole range of DA. Relative displacement is shown in the top panel; DA is shown in the bottom panel.

Table 2 Constitutive parameters κ and k_1 for each class of thickness

Class	κ	k_1 (MPa)
0.4–0.5 mm	$0.320\,^{-0.020}_{+0.010}$	$30\,^{+5}_{-10}$
0.5–0.6 mm	$0.310\,^{-0.030}_{+0.020}$	$45\,^{-15}_{-25}$
0.6–0.7 mm	$0.325\,^{-0.010}_{+0.005}$	$80\,^{+25}_{-15}$

parameters have been found such that the displacement data have been fitted on average, while fitting the DA data to cover the whole experimental range. As a representative example, the finite element results with solid lines for the thickness class of 0.6 − 0.7 mm are reported in Fig. 5. In this figure, the pressure increment has been divided by the sample thickness. The three different parameter sets closely reproduce the displacement data while the κ and k_1 parameters have been adjusted with the purpose to fit the entire range of anisotropy.

Table 2 shows the values for parameters κ and k_1 in the form medium curve $^{+\text{upperlimit}}_{-\text{lowerlimit}}$ for all thickness classes.

In all simulations, the parameters C_{10} and k_2 have been set to 7.0×10^{-4} MPa and 2.5 MPa, respectively.

4 Discussions and Conclusions

The aim of this paper is to create an experimental setup to determine the anisotropic properties of chemically treated bovine pericardium membranes. To this purpose a bulge test and a confocal laser scanning have been used simultaneously.

The anisotropy of the tissue has been quantified through the DA index (anisotropy for DA > 0) as the normalized difference between the maximum and minimum principal curvature. The experimental results have shown that the BP samples used in this study have exhibited a nonlinear relationship between displacements and applied pressure which is consistent with the typical stiffening response of all biological tissues; the data collected within each single class of thickness exhibit a relatively low scatter of data: the maximum standard deviation is 33% at the first pressure increment and progressively decreases with the applied pressure. The DA data exhibit a larger scatter within the thickness classes (the highest standard deviation is 66%). As no direct imaging of the collagen network and related dispersion are available, it can be speculated that fiber orientation dispersion might be different in the different patches used in the study with a little effect on the overall pressure-displacement response.

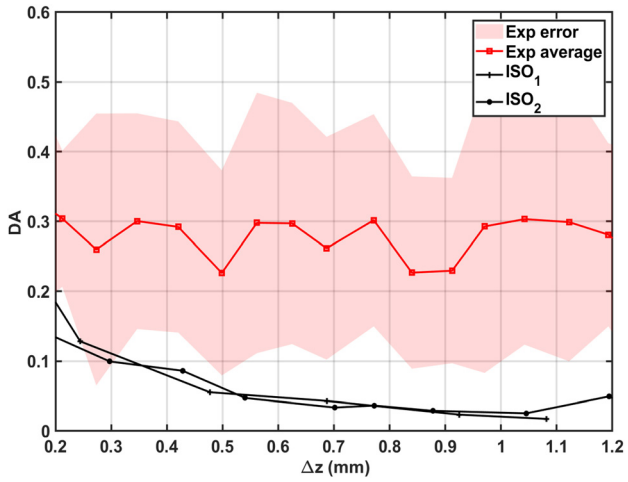

Fig. 6 Comparison between BP (red line) and two isotropic membranes (ISO_1 and ISO_2)

The proposed procedure has proven to be effective in determining tissue anisotropy; indeed, Fig. 6 shows the experimental data found on the BP samples along with the DA value estimated for a bulge test performed on two membranes of rubberlike isotropic material (NBR). As the DA parameter does not exhibit statistical difference among the three thickness classes, in Fig. 6, the three classes are represented as one single group.

Figure 6 shows the comparison between BP and rubberlike material samples DA with respect to maximum displacement on the horizontal axes instead of the applied incremental pressure. This choice is driven by the different pressure levels applied on the rubberlike material samples, which are substantially thinner than the BP samples. The figure clearly shows that the DA calculated on the NBR material is close to zero and substantially smaller than that estimated on the BP membranes. This is more evident at the highest incremental pressure (i.e., the highest displacement Δz); while at the lowest pressure level, DA > 0 is found also for the NBR material. This is due to the effect of the initial configuration found after bolts tightening; the use of the reference configuration is more effective at the highest pressure levels. Figure 7 shows two contour maps of the displacements from three-dimensional-laser scanning (left column) and after interpolation with the 4-th order polynomials (right column). Ellipsoidal shape of the isolines indicates anisotropy of the material (DA = 0.6); while, circular isovalues lines are found on the rubberlike material (DA = 0.04). Zioupos et al. [2] have investigated the BP anisotropy through a bulge test. In particular, the samples have been divided into two groups (apex-base and circumferential), depending on the preferential directions of the fibers with respect to the anatomy. In this work, the diameter of the circular window (41.5 mm) and the pressure (0.67 kPa) which have been applied to the BP are comparable to the ones in the present study. In Ref. [2] the deformed configuration has been identified through Moirè fringes projection determining elliptical profiles for the anisotropic tissue. In order to compare the results found by Zioupos et al. with those found in the present study, the stress–strain data

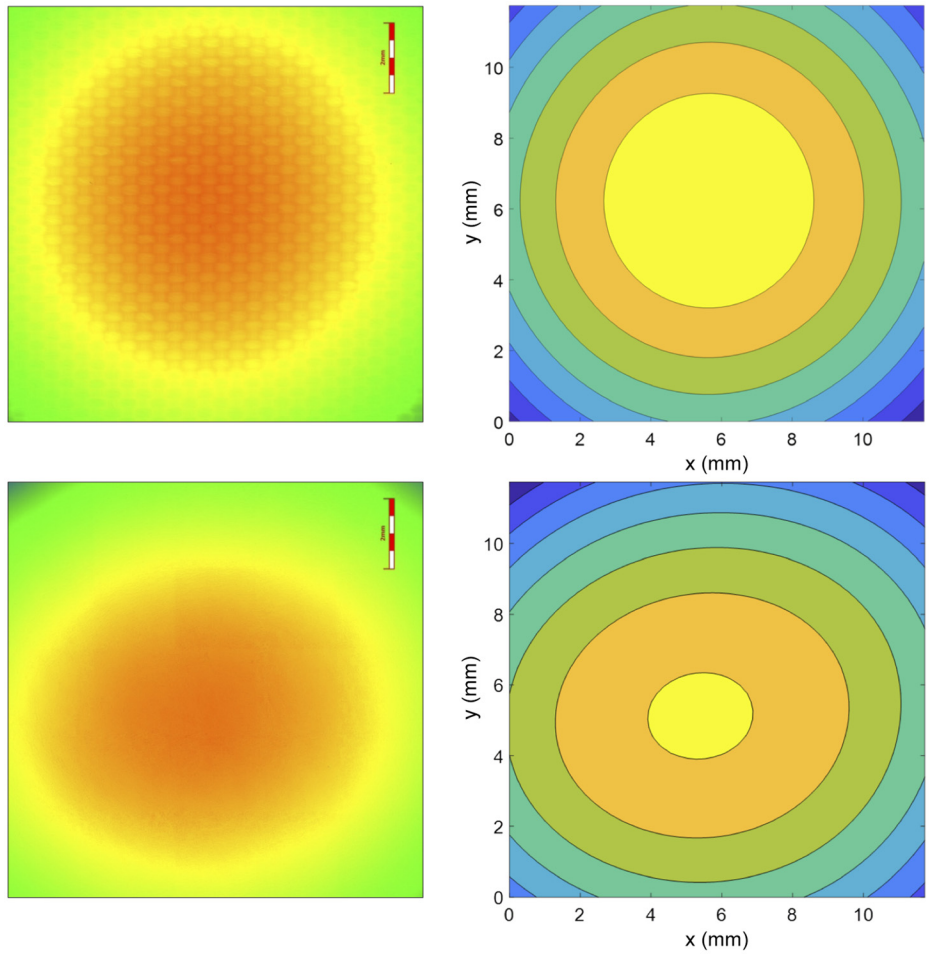

Fig. 7 Displacement contours for the isotropic rubberlike material (DA = 0.04) (top) and for a BP sample (DA = 0.6) (bottom); left column: 3-D topography from confocal laser microscopy (bar size 2 mm); right column: fourth order polynomial interpolation

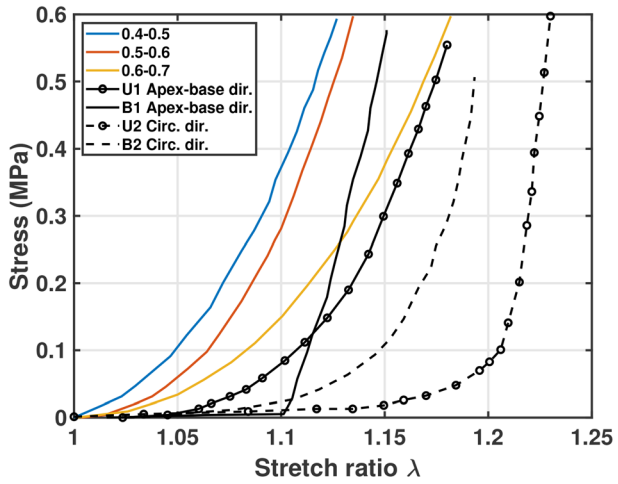

Fig. 8 Comparison between the simulated stress–strain response (solid lines) and the experimental results of Zioupos et al. [2]

found through bulging and through uni-axial and biaxial testing in Ref. [2] are here compared with stress–strain data obtained through the HGO model parameters fitted with our experimental results (see Fig. 8). This comparison shows that along the apex-base direction the stress–strain response found in our study is comparable to that found by Zioupos et al.; with a slightly higher stress found in the present study. Considering the high scattering of data which typically affects experimental tests on biological samples, this comparison is fully satisfactory.

Anisotropy of bovine pericardium has been also investigated by Sacks et al. in Ref. [12] through biaxial tests; although the bulge test is not suitable to span the whole strain range investigated in Ref. [12], the DA found through bulge is consistent with that estimated from the biaxial tests, at least at the representative strain of 2.5%. The validation of the DA parameter through the uni-axial testing has been achieved although the DA obtained through the uni-axial testing is slightly lower than that found through bulge tests. This is owed to the different strain and stress states applied on the tissue in uni-axial tensile tests; while biaxial stretching and bulge tests apply similar strain and stress state to the tissue.

Biaxial stretching of membranes certainly offers a greater flexibility, if compared to the bulge setup, by allowing for different biaxial experimental protocols [20], which guarantees a robust identification of constitutive parameters. Despite the limitations of the bulge test, the experimental setup shown in this study has proven to be sufficiently effective with the great advantage given by the boundary conditions and gripping procedure which are simpler with respect to that required in the biaxial stretching setup, and therefore less prone to experimental errors. Furthermore, one single bulge test is able to identify DA and the principal material directions (the principal axis of the ellipse of confocal images), while uni-axial tests are considerably more expensive as tests along different directions are required. Indeed, in this work only four orientations have been investigated which might be not sufficient to identify the stiffest direction accurately.

The most widely used approach to determine strain field in planar mechanical laboratory tests is the DIC and related advanced techniques (see, for example, Refs. [16,18,21,22]) in which the creation of a pattern, a video camera acquisition system and a software for postprocessing of the images and reconstruction of the deformed tissue are required. In case of three-dimensional deformation modes, like in the bulge testing, a more complex video capturing system and computational analyses are required [23]. The confocal laser microscopy used in this paper returns a high definition height profile of the deformed tissue without further postprocessing, making this technique simpler and faster than the DIC, especially in the experimental setup preparation phase.

The major limitation of this work is the lack of information on the anatomical location and orientation of the BP membranes used in the experiments and consequent lack of information on the fibers architecture and orientation dispersion. Therefore, the DA measured in this work can give information on the average fibers orientation with respect to the boundaries of the tested patches. Another limitation of this study is the irregular shape of the BP membranes after bolts tightening; this problem has been partially overcome by applying an initial pressure $p_0 = 0.1$ kPa to achieve a uniform curvature configuration and using this shape as a reference. Lastly, although the methods have exhibited a high potential in the characterization of the degree of anisotropy of biological membranes, the use of curvatures as second order derivative of the primary variable, i.e., the displacement, has introduced high experimental scatter. Despite this disadvantage, anisotropy has been successfully found in comparison to an isotropic material.

The finite element simulation of the bulge experiments has allowed to assess a range of values of the constitutive parameters of the HGO model. However, the C_{10} and k_2 parameters have been assumed, while a range for the parameter κ and k_1 have been found so to cover the variability of the anisotropy response. A direct comparison of the values of the constitutive parameters with that found by other authors has not been possible. Murdok et al. [24] have identified the parameters of the HGO model for the pericardium; however, they have applied bending tests on thin pericardium membranes which is a loading condition substantially different if compared to the bulge testing. Only a partial validation of the constitutive parameter has been achieved through the comparison of the stress–strain curves obtained through the constitutive parameters selected within the identified range with the uni-axial and biaxial stress–strain data presented in Ref. [2].

In conclusion, this study has laid the groundwork to a better and easier understanding of the characteristics of bovine pericardium so that its microstructure complexity can be effectively exploited in the design and manufacture of BHVs. In addition, the experimental setup and protocol proposed in this study have potentiality to be effective for the characterization, in terms of degree of anisotropy, of other membranous biological tissues.

Data Availability Statement

The datasets generated and supporting the findings of this article are obtainable from the corresponding author upon reasonable request.

References

[1] Whelan, A., Duffy, J., Gaul, R. T., O'Reilly, D., Nolan, D. R., Gunning, P., Lally, C., and Murphy, B. P., 2019, "Collagen Fibre Orientation and Dispersion Govern Ultimate Tensile Strength, Stiffness and the Fatigue Performance of Bovine Pericardium," J. Mech. Behav. Biomed. Mater., **90**(2), pp. 54–60.
[2] Zioupos, P., Barbenel, J. C., and Fisher, J., 1992, "Mechanical and Optical Anisotropy of Bovine Pericardium," Med. Biol. Eng. Comput., **30**(1), pp. 76–82.
[3] Burriesci, G., Howard, I. C., and Patterson, E. A., 1999, "Influence of Anisotropy on the Mechanical Behaviour of Bioprosthetic Heart Valves," J. Med. Eng. Technol., **23**(6), pp. 203–215.
[4] Whelan, A., Williams, E., Nolan, D. R., Murphy, B., Gunning, P. S., O'Reilly, D., and Lally, C., 2021, "Bovine Pericardium of High Fibre Dispersion Has High Fatigue Life and Increased Collagen Content; Potentially an Untapped Source of Heart Valve Leaflet Tissue," Ann. Biomed. Eng., **49**(3), pp. 1022–1032.
[5] Sellaro, T. L., Hildebrand, D., Lu, Q., Vyavahare, N., Scott, M., and Sacks, M. S., 2007, "Effects of Collagen Fiber Orientation on the Response of Biologically Derived Soft Tissue Biomaterials to Cyclic Loading," J. Biomed. Mater. Res., Part A, **80A**(1), pp. 194–205.
[6] Sacks, M. S., and Chuong, C. J., 1998, "Orthotropic Mechanical Properties of Chemically Treated Bovine Pericardium," Ann. Biomed. Eng., **26**(5), pp. 892–902.
[7] Whelan, A., Williams, E., Fitzpatrick, E., Murphy, B. P., Gunning, P. S., O'Reilly, D., and Lally, C., 2021, "Collagen Fibre-Mediated Mechanical Damage Increases Calcification of Bovine Pericardium for Use in Bioprosthetic Heart Valves," Acta Biomater., **128**(7), pp. 384–392.
[8] Yanfei, C., Shigang, A., Jingda, T., Yongmao, P., Liqun, T., and Daining, F., 2017, "Characterizing the Viscoelastic Properties of Hydrogel Thin Films by Bulge Test," ASME J. Appl. Mech., **84**(6), p. 061995.

[9] Paez, J. M. G., Jorge, E., Rocha, A., Maestro, M., Castillo-Olivares, J. L., Millan, I., Carrera, A., et al., 2002, "Mechanical Effects of Increases in the Load Applied in Uniaxial and Biaxial Tensile Testing: Part i. calf Pericardium," J. Mater. Sci.: Mater. Med., **13**(4), pp. 381–388.
[10] Caballero, A., Sulejmani, F., Martin, C., Pham, T., and Sun, W., 2017, "Evaluation of Transcatheter Heart Valve Biomaterials: Biomechanical Characterization of Bovine and Porcine Pericardium," J. Mech. Behav. Biomed. Mater., **75**(11), pp. 486–494.
[11] Liao, J., Yang, L., Grashow, J., and Sacks, M. S., 2005, "Molecular Orientation of Collagen in Intact Planar Connective Tissues Under Biaxial Stretch," Acta Biomater., **1**(1), pp. 45–54.
[12] Sacks, M. S., Chuong, C., and More, R., 1994, "Collagen Fiber Architecture of Bovine Pericardium," ASAIO J., **40**(3), pp. M632–M637.
[13] Labrosse, M. R., Jafar, R., Ngu, J., and Boodhwani, M., 2016, "Planar Biaxial Testing of Heart Valve Cusp Replacement Biomaterials: Experiments, Theory and Material Constants," Acta Biomater., **45**(11), pp. 303–320.
[14] Cavinato, C., Helfenstein-Didier, C., Olivier, T., Du Roscoat, S. R., Laroche, N., and Badel, P., 2017, "Biaxial Loading of Arterial Tissues With 3D in Situ Observations of Adventitia Fibrous Microstructure: A Method Coupling Multi-Photon Confocal Microscopy and Bulge Inflation Test," J. Mech. Behav. Biomed. Mater., **74**(10), pp. 488–498.
[15] Jayyosi, C., Coret, M., and Bruyère-Garnier, K., 2016, "Characterizing Liver Capsule Microstructure Via in Situ Bulge Test Coupled With Multiphoton Imaging," J. Mech. Behav. Biomed. Mater., **54**(2), pp. 229–243.
[16] Whelan, A., O'Brien, G., Szagdaj, A., O'Reilly, D., and Lally, C., 2021, "Investigation Into Early Stage Fatigue-Damage Accumulation in Glutaraldehyde-Fixed Bovine Pericardium Using a Novel Equibiaxial Bulge Inflation System," J. Mech. Behav. Biomed. Mater., **121**, p. 104588.
[17] Sander, E. A., Stylianopoulos, T., Tranquillo, R. T., and Barocas, V. H., 2009, "Image-Based Biomechanics of Collagen-Based Tissue Equivalents," IEEE Eng. Med. Biol. Mag., **28**(3), pp. 10–18.
[18] Boyce, B. L., Grazier, J. M., Jones, R. E., and Nguyen, T. D., 2008, "Full-Field Deformation of Bovine Cornea Under Constrained Inflation Conditions," Biomaterials, **29**(28), pp. 3896–3904.
[19] Gasser, T. C., Ogden, R. W., and Holzapfel, G. A., 2006, "Hyperelastic Modelling of Arterial Layers With Distributed Collagen Fibre Orientations," J. R. Soc. Interface, **3**(6), pp. 15–35.
[20] Witzenburg, C. M., and Barocas, V. H., 2016, "A Nonlinear Anisotropic Inverse Method for Computational Dissection of Inhomogeneous Planar Tissues," Comput. Methods Biomech. Biomed. Eng., **19**(15), pp. 1630–1646.
[21] Sutton, M. A., Orteu, J.-J., and Schreier, H. W., 2009, *Image Correlation for Shape, Motion and Deformation Measurements: Basic Concepts, Theory and Applications*, Springer, New York.
[22] Pyne, J. D., Genovese, K., Casaletto, L., and Vande Geest, J. P., 2014, "Sequential-Digital Image Correlation for Mapping Human Posterior Sclera and Optic Nerve Head Deformation," ASME J. Biomech. Eng., **136**(2), pp. 02–021002.
[23] Solav, D., Moerman, K. M., Jaeger, A. M., Genovese, K., and Herr, H. M., 2018, "MultiDIC: An Open-Source Toolbox for Multi-View 3D Digital Image Correlation," IEEE Access, **6**, pp. 30520–30535.
[24] Murdock, K., Martin, C., and Sun, W., 2018, "Characterization of Mechanical Properties of Pericardium Tissue Using Planar Biaxial Tension and Flexural Deformation," J. Mech. Behav. Biomed. Mater., **77**(1), pp. 148–156.